Gd-EOB-DTPA-enhanced MR findings in chemotherapy-induced sinusoidal obstruction syndrome in colorectal liver metastases

Ying Ding, Sheng-xiang Rao ⓘ**, Wen-tao Wang, Cai-zhong Chen, Ren-chen Li and Mengsu Zeng**

Abstract

Background: We assessed the clinical presentations, biomarkers, and Gd-EOB-DTPA-enhanced MRI features that were associated with oxaliplatin-induced sinusoidal obstruction syndrome (SOS) to detect chemotherapy-associated SOS in a timely manner.

Methods: Fifty-seven patients who underwent oxaliplatin-based chemotherapy and Gd-EOB-DTPA-enhanced MRI were included. Post-oxaliplatin heterogeneity in liver parenchyma was scored on a grading scale of 0 to 3. Abnormal clinical findings, including splenomegaly, hepatomegaly, gall bladder wall thickening, and hepatic vein narrowing, were also assessed. Additionally, alanine transaminase (ALT) levels, aspartate aminotransferase (AST) levels, and platelet counts were measured.

Results: For SOS, 21 patients were scored grade 0, 24 were grade 1, seven were grade 2, and five were grade 3. Hepatomegaly, splenomegaly, gall bladder wall thickening, and hepatic vein narrowing were significantly correlated with the grade for non-tumorous hepatic parenchymal heterogeneity. For laboratory findings, ALT and AST levels, the AST-to-platelet ratio index score, and platelet counts were significantly associated with a high grade ($\geq$2) of non-tumorous hepatic parenchymal heterogeneity.

Conclusions: We assessed the clinical presentations, biomarkers, and Gd-EOB-DTPA-enhanced MRI features that were associated with oxaliplatin-induced sinusoidal obstruction syndrome (SOS) to detect chemotherapy-associated SOS in a timely manner. Additionally, specific laboratory findings were significantly associated with a high grade ($\geq$2).

Department of Radiology, Zhongshan Hospital of Fudan University, Shanghai, China

Corresponding author:
Sheng-xiang Rao, Department of Radiology, Zhongshan Hospital of Fudan University; Shanghai Institute of Medical Imaging; Department of Medical Imaging, Shanghai Medical College, Fudan University; No. 138, Fenglin Road, Xuhui District, Shanghai, China, 200032.
Email: raoxray@163.com

Background

Synchronous and metachronous liver metastases are found in 20% to 25% and 35% to 55%, respectively, of patients with advanced colorectal cancer.[1,2] Surgical resection of hepatic metastases is the standard treatment in resectable disease, and this approach achieves a 30% to 40% increase in the 5-year survival rate.[3,4] However, 80% of patients with liver metastasis at the same time of diagnosis cannot undergo surgical resection because the amount of liver metastasis or the lesion in the liver is too large.[5] Recent advances in chemotherapeutic regimens have led to the common use of perioperative thermotherapy in advanced colorectal cancer. This approach improves progression-free survival in patients with resectable disease and allows for radical surgical resection in patients with initially unresectable colorectal liver metastasis.[6,7]

Oxaliplatin-based chemotherapy is the first-choice treatment and an essential part of chemotherapeutic regimens for advanced colorectal cancer.[8,9] However, despite its considerable benefits, liver damage caused by long-term chemotherapy has arisen as a new clinical problem in colorectal cancer. Recently, the frequency of chemotherapy-associated sinusoidal obstruction syndrome (SOS) has increased in colorectal cancer, in which its incidence is between 42% and 51%.[10] This hepatotoxicity impairs hepatic function, increases the amount of bleeding that occurs during surgery and increases morbidity and mortality after liver resection.

Thus, detecting SOS is important. In addition, oxaliplatin, the main chemical therapy used in colorectal cancer patients, has been reported to be a major contributor to SOS development and is associated with a high incidence of SOS ranging from 51% to 79%.[11] However, chemotherapy-associated SOS is usually asymptomatic.[12] Severe SOS may be associated with the following signs: hepatomegaly with pain, splenomegaly, ascites, hepatic vein narrowing (HVN), and gall bladder wall thickening.[13] The clinical factors and biomarkers that might indicate oxaliplatin-induced SOS have been widely investigated.[14] However, few studies have reported the imaging features of oxaliplatin-induced SOS in the liver.

Gadolinium ethoxybenzyl diethylenetriamine pentaacetic acid (Gd-EOB-DTPA) is a hepatocyte-sensitive magnetic resonance imaging (MRI) contrast medium that can be used to evaluate the hepatobiliary phase (HBP). It is increasingly used to detect and evaluate liver lesions.[15,16] If a lesion has normal functional hepatocytes, it will take up Gd-EOB-DTPA and show iso-/hyperintensity on HBP. In addition, previous studies have shown that patients with liver dysfunction present with reduced liver parenchymal enhancement when using Gd-EOB-DTPA-enhanced MRI in HBP.[17] Thus, SOS should appear as diffuse and heterogeneous hypointensity in the HBP.[18] Shin et al.[19] reported that when CT examination was used in the portal venous phase, a reduction in hepatic parenchymal attenuation was observed following

neoadjuvant therapy, and SOS may be associated with this change. The authors suggested that SOS may have caused sinusoid congestion and thereby delayed contrast agent inflow. However, few papers have explored the use of Gd-EOB-DTPA-enhanced MRI in chemotherapy-induced SOS in colorectal liver metastases. Most studies have reported that SOS increases preoperative morbidity and mortality and post-operative liver failure.[20,21] It is, therefore, very important to increase our understanding of the Gd-EOB-DTPA-enhanced MRI features and clinical presentations of this condition to optimize patient care in individuals with oxaliplatin-induced SOS.

The purpose of our study was to assess clinical presentations, biomarkers, and Gd-EOB-DTPA-enhanced MR imaging features on oxaliplatin-induced SOS. In addition, we also studied inter-observer agreement in these signs.

Methods

Patients

This retrospective study was approved by the Institutional Review Board at our hospital, and the requirement for informed consent was waived. A computerized database search was performed at our institution between March 2011 and December 2017. The inclusion criteria were as follows: (a) patients who had colorectal cancer and underwent more than three sequential oxaliplatin-based chemotherapeutic regimens; (b) patients who underwent a Gd-EOB-DTPA-enhanced MRI examination; (c) patients with no previous oncologic treatment or liver resection; (d) patients with no other diffuse liver disease, such as primary sclerosing cholangitis and primary biliary cirrhosis; and (e) patients who underwent liver biopsy. The exclusion criterion was as follows: more than ten hepatic metastases or a largest metastasis with a diameter greater than 5 cm. Patients with large-volume metastases were excluded because the presence of a relatively small volume of non-tumorous liver parenchyma can alter parenchymal perfusion.

Imaging protocol

All patients underwent an MRI examination using a 1.5-T superconducting magnet 18 (Magnetom Aera, Siemens Medical solutions, Erlangen, Germany) that was equipped with phased-array coils. After the contrast agent, Gd-EOB-DTPA (Primovist®; Bayer-Schering Pharma AG, Berlin, Germany), was administered, dynamic contrast-enhanced (DCE)-MRI was performed using a three-dimensional T1-weighted gradient echo sequence (volumetric interpolated breath-hold examination, VIBE) with the fat-suppression technique. The whole liver and part of the bilateral kidneys were included. The following baseline MRI parameters were used: repetition time millisecond/echo time millisecond, 3.47/1.36; flip angle, 10°; matrix, 320×195; field of view, 380 to 400×300 to 324 mm; slab thickness, 21.6 mm resulting in an interpolated 3-mm section thickness; and bandwidth, 400 Hz/pixel. A parallel imaging technique (R factor of 2) was performed using generalized autocalibrating partially parallel acquisition (GRAPPA). The contrast medium dose was 0.025 mmol/kg. The contrast was rapidly administered manually (at a rate of nearly 1.5 mL/s) by one investigator through a 20-gauge intravenous catheter placed in a cubical or cephalic vein. Immediately afterward, a 20-mL saline flush was administered at the same injection rate. Arterial phase acquisition was triggered automatically when the contrast medium reached the ascending aorta. For subsequent acquisitions, dynamic T1-weighted MRI was performed at

approximately 60 seconds (the portal venous phase) and approximately 90 seconds (the delay phase). In addition, HBP acquisition (20 minutes after contrast media administration) was performed.

Imaging analysis

Two radiologists with more than 10 years of experience in abdominal MRI retrospectively and separately analysed the images. These investigators were blinded to the clinical information. All data were transferred to a workstation (Leonardo, Siemens, Erlangen, Germany) to be evaluated.

Based on the published literature and our own experience, evocative signs of SOS were sought in the portal venous phase and HBP of MRI. Non-tumorous hepatic parenchymal heterogeneity was graded as follows: grade 0 (absent or negligible); grade 1, light (mild heterogeneity); grade 2, moderate (not reaching the whole liver); and grade 3, severe (affecting the entire liver). The following abnormal clinical findings were also assessed: splenomegaly (>130 mm in the coronal plane), hepatomegaly (>140 mm in the coronal plane passing through the portal vein), gall bladder wall thickening (>3 mm), and HVN (measured 1 cm from the superior vena cava).

Laboratory findings

Alanine transaminase (ALT) levels, aspartate aminotransferase (AST) levels, and platelet counts were measured in each patient within 1 week of the MRI examination. The AST-to-platelet ratio index score, an independent predictive factor for severe SOS, was calculated in accordance with the definition presented in Wai et al.,[22] as follows: (AST/ULN)/PC × 100, where ULN is the upper limit of normal AST levels (45 IU/L), and PC is the platelet count in 10^9 cells per litre.

Statistics

All statistical analyses were performed using MedCalc (MedCalc for Windows, version 11.5.0.0, www.medcalc.be). Differences with a p value that were smaller than 0.05 were considered to be statistically significant. The normality of the variables' distribution was established using the Shapiro–Wilk test. Clinical signs were compared as SOS grades using the Student's t-test when normally distributed or the Mann–Whitney U test when not normally distributed. Laboratory findings were examined and compared in high-grade SOS individuals using the Wilcoxon signed rank test. Inter-observer agreement between the two radiologist who scored SOS was analysed using Kappa statistics was as follows: Kappa values <0.20 indicated poor agreement, 0.21 to 0.40 indicated fair agreement, 0.41 to 0.60 indicated moderate agreement, 0.61 to 0.80 indicated good agreement, and >0.81 indicated excellent agreement.

Results

Patients

The final study group comprised 57 patients with an age range of 33 to 81 years (mean age, 56 years), and 35 of the 57 patients were men (age range, 33–81 years; mean age, 63 years), while 22 were women (age range, 45–69 years; mean age, 52 years). A flow chart showing the study population is presented in Figure 1.

Inter-observer agreement

Inter-observer agreement between the two radiologists who scored the severity based on Gd-EOB-DTPA-enhanced MRI findings was excellent at the HBP (k = 0.83, 95% confidence interval: 0.79, 0.87). Thus, the consensus severity scores were used in the data analysis.
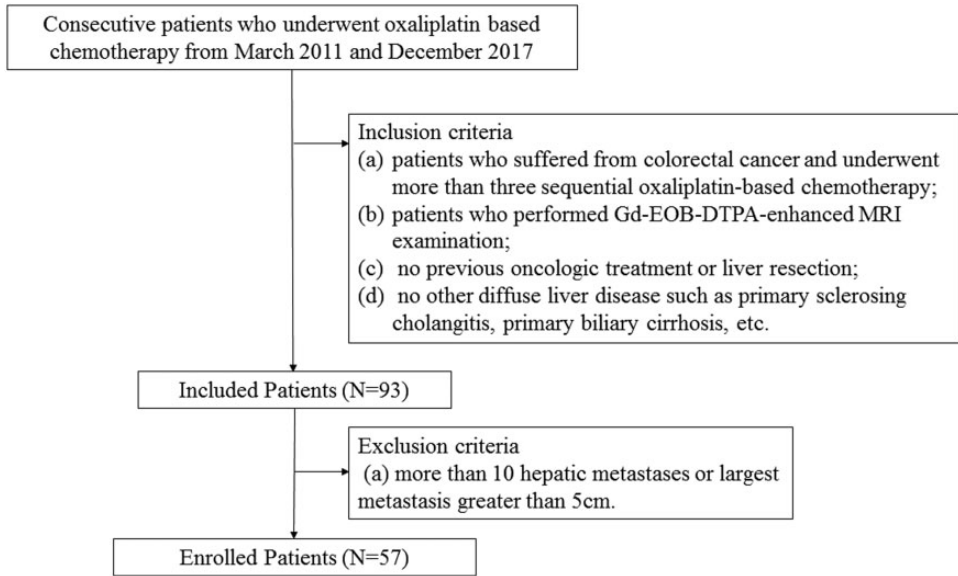
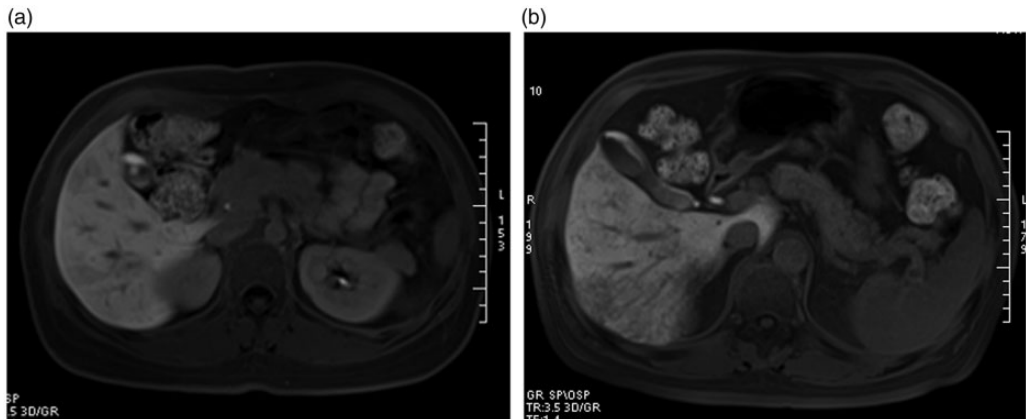Figure 1. A flow chart representing the enrolment of the study population.

Figure 2. a: Gd-EOB-DTPA-enhanced MRI showing a hepatic distribution that was diffuse hypointensity in the liver parenchyma at HBP. b: Peripheral hypointensity was observed in the liver parenchyma at HBP.

Grading non-tumorous hepatic parenchymal heterogeneity

Based on the consensus review, SOS signs indicated a grade of 0 in 21 patients (36.8%), a grade of 1 in 24 patients (42.1%), a grade of 2 in seven patients (12.3%), and a grade of 3 in five patients (8.8%). Among these patients, hepatic distribution was diffuse in four patients (7.0%), peripheral in ten patients (17.54%), and multifocal in 22 patients (38.60%) (Figure 2). Hepatomegaly, splenomegaly, gall bladder wall thickening, and HVN were significantly correlated with the grades that were assigned for non-tumorous hepatic

parenchymal heterogeneity (p = 0.02, p < 0.0001, p = 0.009, and p = 0.007, respectively). For the laboratory findings, AST levels, ALT levels, AST-to-platelet ratio index scores, and platelet counts were significantly associated with a high grade (≥2) for non-tumorous hepatic parenchymal heterogeneity (p = 0.007, p = 0.03, p = 0.009, and p = 0.006, respectively).

Imaging findings during Gd-EOB-DTPA-enhanced MRI

Table 1 summarizes the imaging findings and their correlations with grades for non-tumorous hepatic parenchymal heterogeneity in the initial examinations. Hepatomegaly (rho = 0.413, p = 0.02), splenomegaly (rho = 0.458, p < 0.0001), and gall bladder wall thickening (rho = 0.326, p = 0.009) were significantly and positively correlated with SOS grade for non-tumorous hepatic parenchymal heterogeneity. In addition, HVN (rho = −0.302, p = 0.007) was negatively correlated with changes in SOS grades for non-tumorous hepatic parenchymal heterogeneity.

Laboratory findings

Table 2 shows the results of Spearman's correlation tests of laboratory findings in individuals with a high grade (≥2) and non-tumorous hepatic parenchymal heterogeneity. High AST levels (rho = 0.312, p = 0.007), high ALT levels (rho = 0.210, p = 0.03), a high AST-to-platelet ratio index score (rho = 0.275, p = 0.009), and a low platelet count (rho = −0.289, p = 0.006) were significantly associated with a high grade (≥2) for non-tumorous hepatic parenchymal heterogeneity.

Discussion

The goal of this study was to assess the clinical presentations oxaliplatin-induced SOS

Table 1. Mean values (±standard deviation) and correlations between imaging findings and SOS grades for non-tumorous hepatic parenchymal heterogeneity.

	Patient Numbers	Mean Values	rho	95%CI	p value
Hepatomegaly (mm)	50	159.71 ± 32.3	0.413	0.312–0.433	0.02
Splenomegaly (mm)	26	138.9 ± 23.7	0.458	0.334–0.571	<0.0001
GWT (mm)	12	3.3 ± 0.5	0.326	0.275–0.431	0.009
HVN (mm)	12	4.2 ± 0.4	−0.302	−0.287−−0.314	0.007

SOS, sinusoidal obstruction syndrome; 95%CI, 95% confidence interval for rho.
GWT, gall bladder wall thickening; HVN, hepatic vein narrowing.

Table 2. Results of Spearman's correlation tests of laboratory findings in individuals with a high grade (≥2) for non-tumorous hepatic parenchymal heterogeneity.

	ALT (IU/L) (n = 12)	AST (IU/L) (n = 12)	Platelet count (10^3/μL) (n = 12)	AST-to-platelet ratio index Score (n = 12)
rho	0.312	0.210	−0.289	0.275
95%CI	0.198–0.452	0.176–0.315	−0.179−−0.413	0.190–0.402
p value	0.007	0.03	0.006	0.009

95%CI, 95% confidence interval for rho; ALT, alanine transaminase; AST, aspartate aminotransferase.

on Gd-EOB-DTPA-enhanced MRI. SOS manifests as diffuse liver damage that causes liver congestion. It was first described in 1920 in association with the ingestion of Senecio tea containing the natural toxins pyrrolizidine alkaloids.[23] It is an idiosyncratic adverse effect of chemotherapeutic agents that is histologically characterized by sinusoidal dilatation accompanied by peliosis, nodular regenerative hyperplasia, and fibrosis.

Several studies have shown that SOS increases the risk of major hepatectomy and perioperative bleeding, and it also increases the use of transfusions.[24,25] It was previously called hepatic veno-occlusive disease (VOD), and a recent study indicated that the primary site of damage in VOD is centrilobular (zone 3 of the liver parenchyma) sinusoidal endothelial cells.[26] However, in normal liver parenchyma, the expression of organic anion transporting polypeptide1B3 (OATP1B3), the main uptake transporter of Gd-EOB-DTPA, is observed predominantly in centrilobular hepatocytes (zone 3). Thus, because hepatocytes are damaged in SOS patients, OAPT1B3 expression was remarkably reduced and we observed hypointensity at HBP in patients with SOS. In our study, we found that 21 patients were grade 0, 24 were grade 1, seven were grade 2, and five were grade 3. In addition, the hepatic distribution was diffuse in four patients (7.0%), peripheral in ten patients (17.54%), and multifocal in 22 patients (38.60%). Additionally, Shin et al.[19] showed that the presence of reticular hypointensity at HBP on Gd-EOB-DTPA-enhanced MRI was a highly specific indicator of a diagnosis of SOS. Therefore, they proposed that Gd-EOB-DTPA-enhanced MRI may be a very useful tool for detecting SOS at a relatively early stage.

Hepatomegaly, splenomegaly, thickening of the gall bladder walls, and narrowing of the hepatic vein are mainly described in cases of SOS that result from exposure to pyrrolizidine alkaloids and hematopoietic stem cell transplantation. In our study, all four of these findings were significantly correlated with the grade for non-tumorous hepatic parenchymal heterogeneity (p = 0.02, p < 0.0001, p = 0.009, and p = 0.007, respectively); however, they were not all specific. For example, hepatomegaly was observed in patients with infectious hepatitis, while increased spleen size has been reported as a predictor of sinusoidal injury. The results of a previous CT-based study showed that right hepatic diameter was significantly smaller in patients with SOS compared with those with graft-versus-host disease.[27] The authors, therefore, suggested that a right hepatic vein measuring less than 4.5 mm in diameter was highly suggestive of SOS. Finally, gall bladder wall thickening is most likely caused by an increase in resistance to venous inflow and indicates the primary vascular nature of SOS.

In addition to the clinical presentation of features on Gd-EOB-DTPA-enhanced MRI, a variety of biochemical parameters have been found to predict the presence and severity of chemotherapy-induced SOS, as shown in several studies.[28,29] We found that elevated AST levels, elevated ALT levels, a high AST-to-platelet ratio index score, and a low platelet count were significantly associated with a high grade (≥2) for non-tumorous hepatic parenchymal heterogeneity. These results are consistent with those that are presented in previous studies showing that elevated liver enzyme levels and a low platelet count are likely to be associated with SOS.[30]

There are some limitations to our study. First, the retrospective nature of our study meant that we could not avoid sampling bias. Second, the sample size was relatively small, and this might have affected the results.

Conclusions

Gd-EOB-DTPA-enhanced MRI findings revealed the clinical features of oxaliplatin-induced SOS. It has the potential to be the biomarker for diagnosing oxaliplatin-induced SOS in its early stage. Finally, we identified laboratory findings that were significantly associated with a high grade ($\geq$2).

List of abbreviations

SOS, sinusoidal obstruction syndrome
HVN, hepatic vein narrowing
Gd-EOB-DTPA, gadolinium ethoxybenzyl diethylenetriamine pentaacetic acid
MRI, magnetic resonance imaging
HBP, hepatobiliary phase
DCE, dynamic contrast-enhanced
VIBE, volumetric interpolated breath-hold examination
GRAPPA, generalized auto-calibrating partially parallel acquisition
ALT, alanine transaminase
AST, aspartate aminotransferase
VOD, veno-occlusive disease
OATP1B3, organic anion transporting polypeptide1B3

Author contribution

1. guarantor of integrity of the entire study: Sheng-Xiang Rao
2. study concepts and design: Meng-Su Zeng
3. literature research: Ying Ding
4. clinical studies: Ying Ding
5. experimental studies/data analysis: Caizhong Chen; Renchen Li
6. statistical analysis: Ying Ding; Wen-tao Wang
7. manuscript preparation: Ying Ding
8. manuscript editing: Sheng-Xiang Rao

Availability of data and materials

The datasets used and analysed during the current study are available from the corresponding author on reasonable request.

Consent for publication

The requirement for informed consent was waived.

Declaration of conflicting interest

Ethics approval and consent to participate

This retrospective study was approved by the Institutional Review Board at our hospital, and the requirement for informed consent was waived.

Funding

ORCID iD

Sheng-xiang Rao (ID) https://orcid.org/0000-0001-7722-8327

References

1. Siegel R, Naishadham D and Jemal A. Cancer statistics. *CA Cancer J Clin* 2014; 64: 9–29.
2. Seront E and Van den Eynde M. Liver-directed therapies: Does it make sense in the current therapeutic strategy for patients with confined liver colorectal metastases? *Clin Colorectal Cancer* 2012; 11: 177–184.

3. Parau A and Vlad L. Colorectal cancer with liver metastases–is there a chance for cure? *Chirurgia (Bucur)* 2014; 109: 161–167.

4. Blackham AU, Russell GB, Stewart JH 4th, et al. Metastatic colorectal cancer: Survival comparison of hepatic resection versus cytoreductive surgery and hyperthermic intraperitoneal chemotherapy. *Ann Surg Oncol* 2014; 21: 2667–2674.

5. Ahmed S and Eng C. Neoadjuvant strategies: Locally advanced rectal cancer. *Clin Colon Rectal Surg* 2017; 30: 383–386.

6. Dwek MR, Rixon L, Simon A, et al. Examining the effects of adjuvant chemotherapy on cognition and the impact of any cognitive impairment on quality of life in colorectal cancer patients: Study protocol. *BMC Psychol* 2015; 3: 43.

7. Bosset JF, Calais G, Mineur L, et al. Fluorouracil-based adjuvant chemotherapy after preoperative chemoradiotherapy in rectal cancer: Long-term results of the EORTC 22921 randomised study. *Lancet Oncol* 2014; 15: 184–190.

8. Nishioka Y, Moriyama J, Matoba S, et al. Prognostic impact of adjuvant chemotherapy after hepatic resection for synchronous and early metachronous colorectal liver metastases. *Dig Surg* 2017; 35: 187–195. doi: 10.1159/000478791. [Epub ahead of print]

9. Mizushima T, Fukunaga M, Sueda T, et al. Phase I/II study of bi-weekly XELIRI plus bevacizumab treatment in patients with metastatic colorectal cancer resistant to oxaliplatin-based first-line chemotherapy. *Cancer Chemother Pharmacol* 2017; 80: 81–90.

10. Yoneda N, Matsui O, Ikeno H, et al. Correlation between Gd-EOB-DTPA-enhanced MR imaging findings and OATP1B3 expression in chemotherapy-associated sinusoidal obstruction syndrome. *Abdom Imaging* 2015; 40: 3099–3103.

11. Bilchik AJ, Poston G, Curley SA, et al. Neoadjuvant chemotherapy for metastatic colon cancer: A cautionary note. *J Clin Oncol* 2005; 23: 9073–9078.

12. Duwe G, Knitter S, Pesthy S, et al. Hepatotoxicity following systemic therapy for colorectal liver metastases and the impact of chemotherapy-associated liver injury on outcomes after curative liver resection. *Eur J Surg Oncol* 2017; 43: 1668–1681.

13. Khan AZ, Morris-Stiff G and Makuuchi M. Patterns of chemotherapy-induced hepatic injury and their implications for patients undergoing liver resection for colorectal liver metastases. *J Hepatobiliary Pancreat Surg* 2009; 16: 137–144.

14. Park S, Kim HY, Kim H, et al. Changes in noninvasive liver fibrosis indices and spleen size during chemotherapy: Potential markers for oxaliplatin-induced sinusoidal obstruction syndrome. *Medicine (Baltimore)* 2016; 95: e2454.

15. Siegelman ES and Chauhan A. MR characterization of focal liver lesions: Pearls and pitfalls. *Magn Reson Imaging Clin N AM* 2014; 22: 295–313.

16. Choi JY, Lee JM and Sirlin CB. CT and MR imaging diagnosis and staging of hepatocellular carcinoma: Part I. Development, growth, and spread: Key pathologic and imaging aspects. *Radiology* 2014; 272: 635–654.

17. Saito K, Ledsam J, Sourbron S, et al. Measuring hepatic functional reserve using low temporal resolution Gd-EOB-DTPA dynamic contrast-enhanced MRI: A preliminary study comparing galactosyl human serum albumin scintigraphy with indocyanine green retention. *Eur Radiol* 2014; 24: 112–119.

18. Han NY, Park BJ, Yang KS, et al. Hepatic parenchymal heterogeneity as a maker for oxaliplatin-induced sinusoidal obstruction syndrome: Correlation with treatment response of colorectal cancer liver metastases. *Am J Roentagenol* 2017; 209: 1039–1045.

19. Shin NY, Kim MJ, Lim JS, et al. Accuracy of gadoxetic acid-enhanced magnetic resonance imaging for the diagnosis of sinusoidal obstruction syndrome in patients with chemotherapy-treated colorectal liver metastases. *Eur Radiol* 2012; 22: 864–871.

20. Tamandl D, Klinger M, Eipeldauer S, et al. Sinusoidal obstruction syndrome impairs long-term outcome of colorectal liver metastases treated with resection after neoadjuvant chemotherapy. *Ann Surg Oncol* 2011; 18: 421–430.

21. Cayet S, Pasco J, Dujardin F, et al. Diagnostic performance of contrast-enhanced CT-scan in sinusoidal obstruction syndrome induced by chemotherapy of colorectal liver metastases: Radio-pathological correlation. *Eur J Radiol* 2017; 94: 180–190.

22. Wai CT, Greenson JK, Fontana RJ, et al. A simple noninvasive index can predict both significant fibrosis and cirrhosis in patients with chronic hepatitis C. *Hepatology* 2006; 239: 105–112.

23. Wilmont FC and Robertson GW. Senecio disease, or cirrhosis of the liver due to senecio poisoning. *Lancet* 1920; 196: 848–849.

24. Park SH, Lee SS, Sung JY, et al. Noninvasive assessment of hepatic sinusoidal obstructive syndrome using acoustic radiation force impulse elastography imaging: A proof-of-concept study in rat models. *Eur Radiol* 2018; 28: 2096–2106. doi: 10.1007/s00330-017-5179-z.

25. Coutsouvelis J, Avery S, Dooley M, et al. Defibrotide for the treatment of sinusoidal obstruction syndrome: Evaluation of response to therapy and patient outcomes. *Support Care Cancer* 2018; 26: 947–955.

26. Ni Chonghaile M and Wolownik K. Identification and management: Sinusoidal obstruction syndrome/veno-occlusive disease related to hematopoietic stem cell transplantation. *Clin J Oncol Nurs* 2018; 22: E7–E17.

27. Erturk SM, Mortele KJ, Binkert CA, et al. CT features of hepatic venoocclusive disease and hepatic graft-versus-host disease in patients after hematopoietic stem cell transplantation. *Am J Roentgenol* 2006; 186: 1497–1501.

28. Han NY, Park BJ, Kim MJ, et al. Hepatic parenchymal heterogeneity on contrast-enhanced CT scans following oxaliplatin-based chemotherapy: Natural history and association with clinical evidence of sinusoidal obstruction syndrome. *Radiology* 2015; 276: 766–774.

29. Soubrane O, Brouquet A, Zalinski S, et al. Predicting high grade lesions of sinusoidal obstruction syndrome related to oxaliplatin-based chemotherapy for colorectal liver metastases: Correlation with post-hepatectomy outcome. *Ann Surg* 2010; 251: 454–460.

30. Nakano H, Oussoultzoglou E, Rosso E, et al. Sinusoidal injury increases morbidity after major hepatectomy in patients with colorectal liver metastases receiving preoperative chemotherapy. *Ann Surg* 2008; 247: 118–124.